

HOW DO LANGUAGE MODELS BIND ENTITIES IN CONTEXT?

Jiahai Feng* & Jacob Steinhardt
UC Berkeley

ABSTRACT

To correctly use in-context information, language models (LMs) must bind entities to their attributes. For example, given a context describing a “green square” and a “blue circle”, LMs must bind the shapes to their respective colors. We analyze LM representations and identify the *binding ID mechanism*: a general mechanism for solving the binding problem, which we observe in every sufficiently large model from the Pythia and LLaMA families. Using causal interventions, we show that LMs’ internal activations represent binding information by attaching *binding ID vectors* to corresponding entities and attributes. We further show that binding ID vectors form a continuous subspace, in which distances between binding ID vectors reflect their discernability. Overall, our results uncover interpretable strategies in LMs for representing symbolic knowledge in-context, providing a step towards understanding general in-context reasoning in large-scale LMs.

1 INTRODUCTION

Modern language models (LMs) excel at many reasoning benchmarks, suggesting that they can perform general purpose reasoning across many domains. However, the mechanisms that underlie LM reasoning remain largely unknown (Räuber et al., 2023). The deployment of LMs in society has led to calls to better understand these mechanisms (Hendrycks et al., 2021), so as to know why they work and when they fail (Mu & Andreas, 2020; Hernandez et al., 2021; Vig et al., 2020b).

In this work, we seek to understand *binding*, a foundational skill that underlies reasoning. How humans solve binding, i.e. recognize features of an object as bound to that object and not to others, is a fundamental problem in psychology (Treisman, 1996). Here, we study binding in LMs.

Binding arises any time the LM has to reason about two or more objects of the same kind. For example, consider the following passage involving two people and two countries:

Context: Alice lives in the capital city of France. Bob lives in the capital city of Thailand.
Question: Which city does Bob live in? (1)

In this example the LM has to represent the associations $lives(Alice, Paris)$ and $lives(Bob, Bangkok)$. We call this the *binding problem*—for the predicate *lives*, *Alice* is bound to *Paris* and *Bob* to *Bangkok*. Since predicates are bound in-context, binding must occur in the activations, rather than in the weights as with factual recall (Meng et al., 2022). This raises the question: how do LMs represent binding information in the context such that they can be later recalled?

Overall, our key technical contribution is the identification of a robust general mechanism in LMs for solving the binding problem. The mechanism relies on *binding IDs*, which are abstract concepts that LMs use internally to mark variables in the same predicate apart from variables in other predicates (Fig. 1). Using causal mediation analysis we empirically verify two key properties of the binding ID mechanism (Section 3).

Turning to the structure of binding IDs, we find that binding IDs are represented as vectors which are bound to variables by simple addition (Section 4). Further, we show that binding IDs occupy a subspace, in the sense that linear combinations of binding IDs are still valid binding IDs, even though random vectors are not.

*Correspondence to fjiahai@berkeley.edu

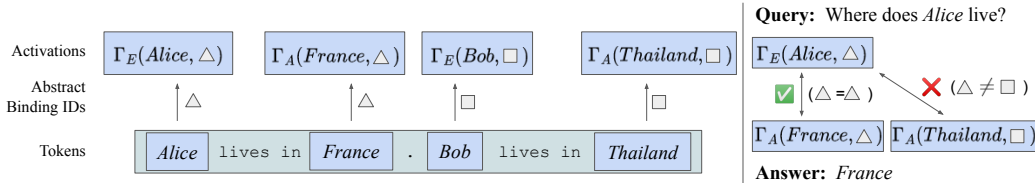


Figure 1: The Binding ID mechanism. The LM learns abstract binding IDs (drawn as triangles or squares) which distinguish between entity-attribute pairs. Binding functions Γ_E and Γ_A bind entities and attributes to their abstract binding ID, and store the results in the activations. To answer queries, the LM identifies the attribute that shares the same binding ID as the queried entity.

Lastly, we find that binding IDs are ubiquitous and transferable (Section 5). They are used by every sufficiently large model in the LLaMA (Touvron et al., 2023) and Pythia (Biderman et al., 2023) families, and their fidelity increases with scale. They are used for a variety of synthetic binding tasks with different surface forms, and binding vectors from one task transfer to other tasks. Finally, we qualify our findings by showing that despite their ubiquity, binding IDs are not universal: we exhibit a question-answering task where an alternate mechanism, “direct binding”, is used instead.

2 PRELIMINARIES

In this section we define the *binding task* and explain causal mediation analysis, our main experimental technique.

Binding task. Formally, the binding task consists of a set of entities \mathcal{E} and a set of attributes \mathcal{A} . An n -entity instance of the binding task consists of a context that is constructed from n entities $e_0, \dots, e_{n-1} \in \mathcal{E}$ and n attributes $a_0, \dots, a_{n-1} \in \mathcal{A}$, and we denote the corresponding context as $\mathbf{c} = \text{ctxt}(e_0 \leftrightarrow a_0, \dots, e_{n-1} \leftrightarrow a_{n-1})$. For a context \mathbf{c} , we use $E_k(\mathbf{c})$ and $A_k(\mathbf{c})$ to denote the k -th entity and the k -th attribute of the context \mathbf{c} , for $k \in [0, n-1]$. We will drop the dependence on \mathbf{c} for brevity when the choice of \mathbf{c} is clear from context.

In the CAPITALS task, which is the main task we study for most of the paper, \mathcal{E} is a set of single-token names, and \mathcal{A} is a set of single-token countries. Quote 1 is an example instance of the CAPITALS task with context $\mathbf{c} = \text{ctxt}(\text{Alice} \leftrightarrow \text{France}, \text{Bob} \leftrightarrow \text{Thailand})$. In this context, E_0 is Alice, A_0 is France, etc.

Given a context \mathbf{c} , we are interested in the model’s behavior when queried with each of the n entities present in \mathbf{c} . For any $k \in [0, n-1]$, when queried with the entity E_k the model should place high probability on the answer matching A_k . In our running example, the model should predict “Paris” when queried with “Alice”, and “Bangkok” when queried with “Bob”.

To evaluate a model’s behavior on a binding task, we sample $N = 100$ contexts. For each context \mathbf{c} , we query the LM with every entity mentioned in the context, which returns a vector of log probabilities over every token in the vocabulary. The *mean log prob* metric measures the mean of the log probability assigned to the correct attribute token. Top-1 accuracy measures the proportion of queries where the correct attribute token has the highest log probability out of all attribute tokens. However, we will instead use the *median-calibrated accuracy* (Zhao et al., 2021), which calibrates the log probabilities with the median log probability before taking the top-1 accuracy. We discuss this choice in Appendix A.

Causality in autoregressive LMs. We utilize inherent causal structure in autoregressive LMs. Let an LM have n_{layers} transformer layers and a d_{model} -dimensional activation space. For every token position p , we use $Z_p \in \mathbb{R}^{n_{\text{layers}} \times d_{\text{model}}}$ to denote the stacked set of internal activations¹ at token p (see Fig. 2a). We refer to the collective internal activations of the context as Z_{context} . In addition, we denote the activations at the token for the k -th entity as Z_{E_k} , and the k -th attribute as Z_{A_k} . We sometimes write $Z_{A_k}(\mathbf{c})$, $Z_{\text{context}}(\mathbf{c})$, etc. to make clear the dependence on the context \mathbf{c} .

¹These are the pre-transformer layer activations, sometimes referred to as the *residual stream*.

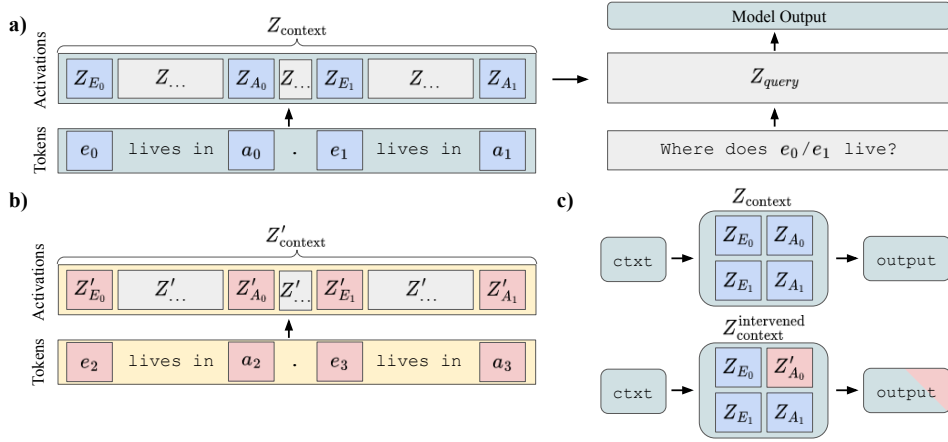


Figure 2: **a)** Causal diagram for autoregressive LMs. From input context $\text{ctxt}(e_0 \leftrightarrow a_0, e_1 \leftrightarrow a_1)$, the LM constructs internal representations Z_{context} . We will mainly study the components of Z_{context} boxed in blue. **b)** A secondary run of the LM on context $\text{ctxt}(e_2 \leftrightarrow a_2, e_3 \leftrightarrow a_3)$ to produce Z'_{context} . **c)** An example intervention where Z_{context} is modified by replacing $Z_{A_0} \rightarrow Z'_{A_0}$ from Z'_{context} .

Fig. 2a shows that Z_{context} contains all the information about the context that the LM uses. We thus study the structure of Z_{context} using *causal mediation analysis*, a widely used tool for understanding neural networks (Vig et al., 2020a; Geiger et al., 2021; Meng et al., 2022). Causal mediation analysis involves substituting one set of activations in a network for another, and we adopt the $/\cdot$ notation (from Mathematica) to denote this. For example, for activations $Z_* \in \mathbb{R}^{n_{\text{layers}} \times d_{\text{model}}}$, and a token position p in the context, $Z_{\text{context}}/\cdot\{Z_p \rightarrow Z_*\} = [Z_0, \dots, Z_{p-1}, Z_*, Z_{p+1}, \dots]$. Similarly, for a context $\mathbf{c} = \text{ctxt}(e_0 \leftrightarrow a_0, \dots, e_{n-1} \leftrightarrow a_{n-1})$, we have $\mathbf{c}/\cdot\{E_k \rightarrow e_*\} = \text{ctxt}(e_0 \leftrightarrow a_0, \dots, e_* \leftrightarrow a_k, \dots, e_{n-1} \leftrightarrow a_{n-1})$.

Given a causal graph, causal mediation analysis determines the role of an intermediate node by experimentally intervening on the value of the node and measuring the model’s output on various queries. For convenience, when the model answers queries in accordance to a context \mathbf{c} , we say that the model *believes*² \mathbf{c} . If there is no context consistent with the language model’s behavior, then we say that the LM is *confused*.

As an example, suppose we are interested in the role of the activations Z_{A_0} in Fig. 2a. To apply causal mediation analysis, we would:

1. Obtain Z_{context} by running the model on the original context \mathbf{c} (which we also refer to as the *target* context) (Fig. 2a)
2. Obtain Z'_{context} by running the model on a different context \mathbf{c}' (i.e. *source* context) (Fig. 2b)
3. Modify Z_{context} by replacing Z_{A_0} from the target context with Z'_{A_0} from the source context (Fig. 2c), while keeping all other aspects of Z_{context} the same, resulting in $Z_{\text{context}}^{\text{intervened}} = Z_{\text{context}}/\cdot\{Z_{A_0} \rightarrow Z'_{A_0}\}$
4. Evaluate the model’s beliefs based on the new $Z_{\text{context}}^{\text{intervened}}$

We can infer the causal role of Z_{A_0} from how the intervention $Z_{\text{context}}/\cdot\{Z_{A_0} \rightarrow Z'_{A_0}\}$ changes the model’s beliefs. Intuitively, if the model retains its original beliefs \mathbf{c} , then Z_{A_0} has no causal role in the model’s behavior on the binding task. On the other hand, if the model now believes the source context \mathbf{c}' , then Z_{A_0} contains all the information in the context. In reality both hypothetical extremes are implausible, and in Section 3 we discuss a more realistic hypothesis.

A subtle point is that we study how different components of Z_{context} store information about the context (and thus influence behavior), and not how Z_{context} itself is constructed. We thus suppress

²We do not claim or assume that LMs actually have beliefs in the sense that humans do. This is a purely notational choice to reduce verbosity.

the causal influence that Z_{A_0} has on downstream parts of Z_{context} (such as Z_{E_1} and Z_{A_1}) by freezing the values of Z_{E_1} and Z_{A_1} in $Z_{\text{context}}^{\text{intervened}}$ instead of recomputing them based on Z'_{A_0} .

3 EXISTENCE OF BINDING IDS

In this section, we first describe our hypothesized binding ID mechanism. Then, we identify two key predictions of the mechanism, factorizability and position independence, and verify them experimentally. We provide an informal argument in Appendix B for why this binding ID mechanism is the only mechanism consistent with factorizability and position independence.

Binding ID mechanism. We claim that to bind attributes to entities, the LM learns abstract binding IDs that it assigns to entities and attributes, so that entities and attributes bound together have the same binding ID (Fig. 1). In more detail, our informal description of the binding ID mechanism is:

1. For entity E_k , encode both the entity E_k and the binding ID k ³ in the activations Z_{E_k} .
2. For attribute A_k , encode both the attribute A_k and the binding ID k in the activations Z_{A_k} .
3. To answer a query for entity E_k , retrieve from Z_{context} the attribute that shares the same binding ID as E_k .

Further, for activations Z_{E_k} and Z_{A_k} , the binding ID and the entity/attribute are the only information they contain that affects the query behavior.

More formally, there are *binding functions* $\Gamma_E(e, k)$ and $\Gamma_A(a, k)$ that fully specify how Z_E and Z_A bind entities/attributes with binding IDs. Specifically, if $E_k = e \in \mathcal{E}$, then we can replace Z_{E_k} with $\Gamma_E(e, k)$ without changing the query behavior, and likewise for Z_A .

More generally, given Z_{context} with entity representations $\Gamma_E(e_0, 0), \dots, \Gamma_E(e_{n-1}, n-1)$ and attribute representations $\Gamma_A(a_0, \pi(0)), \dots, \Gamma_A(a_{n-1}, \pi(n-1))$ for a permutation π , the LM should answer queries according to the context $\mathbf{c} = \text{ctx}(e_0 \leftrightarrow a_{\pi^{-1}(0)}, \dots, e_{n-1} \leftrightarrow a_{\pi^{-1}(n-1)})$. This implies two properties in particular, which we will test in the following subsections:

- **Factorizability:** if we replace Z_{A_k} with $Z_{A'_k}$, then the model will bind E_k to A'_k instead of A_k , i.e. it will believe $\mathbf{c} / \{A_k \rightarrow A'_k\}$. This is because Z'_{A_k} encodes $\Gamma_A(A'_k, k)$ and Z_{A_k} encodes $\Gamma_A(A_k, k)$. Substituting $Z_{A_k} \rightarrow Z_{A'_k}$ will overwrite $\Gamma_A(A_k, k)$ with $\Gamma_A(A'_k, k)$, causing the model to bind E_k to A'_k .
- **Position independence:** if we e.g. swap Z_{A_0} and Z_{A_1} , the model still binds $A_0 \leftrightarrow E_0$ and $A_1 \leftrightarrow E_1$, because it looks up attributes based on binding ID and not position in the context.

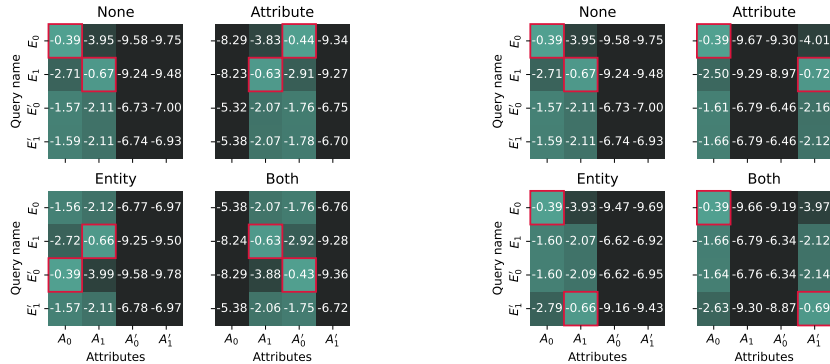
In Section 4, we construct fine-grained modifications to the activation Z that modify the binding ID but not the attributes, allowing us to test the binding hypothesis more directly. In Section 5 we extend this further by showing that binding IDs can be transplanted from entirely different tasks.

3.1 FACTORIZABILITY OF ACTIVATIONS

The first property of Z_{context} we test is *factorizability*. In our claimed mechanism, information is highly localized— Z_{A_k} contains all relevant information about A_k , and likewise for Z_{E_k} . Therefore, we expect LMs that implement this mechanism to have factorizable activations: for any contexts \mathbf{c}, \mathbf{c}' , substituting $Z_{E_k} \rightarrow Z_{E_k}(\mathbf{c}')$ into $Z_{\text{context}}(\mathbf{c})$ will cause the model to believe $\mathbf{c} / \{E_k \rightarrow E'_k\}$, and substituting $Z_{A_k} \rightarrow Z_{A_k}(\mathbf{c}')$ cause the model to believe $\mathbf{c} / \{A_k \rightarrow A'_k\}$.

To test this concretely, we considered the CAPITALS task from Section 2 with $n = 2$ entity-attribute pairs. We computed representations for two contexts $\mathbf{c} = \text{ctx}(e_0 \leftrightarrow a_0, e_1 \leftrightarrow a_1)$ and $\mathbf{c}' = \text{ctx}(e'_0 \leftrightarrow a'_0, e'_1 \leftrightarrow a'_1)$, and used causal mediation analysis (Section 2) to swap representations from the source context \mathbf{c}' into the target context \mathbf{c} . Specifically, we fix $k \in \{0, 1\}$ and intervene on either just the entity ($Z_{E_k} \rightarrow Z'_{E_k}$), just the attribute, neither, or both. We then measure the mean log probs for all possible queries (E_0, E_1, E'_0, E'_1). For instance, swapping A_k with A'_k in Z_{context} should lead A'_k (and not A_k) to have high log-probability when E_k is queried.

³In Fig. 1 we used shapes to denote abstract binding IDs. In the text, we will identify the abstract binding IDs with the integers $\{0, 1, \dots, n-1\}$ so that the k -th entity/attribute has the abstract binding ID k .



(a) Swapping entity/attribute for (E_0, A_0) (b) Swapping entity/attribute for (E_1, A_1)

Figure 3: Factorizability results. Each row corresponds to querying for a particular entity. Plotted are the mean log prob for all four attributes. Highlighted squares are predicted by factorizability.

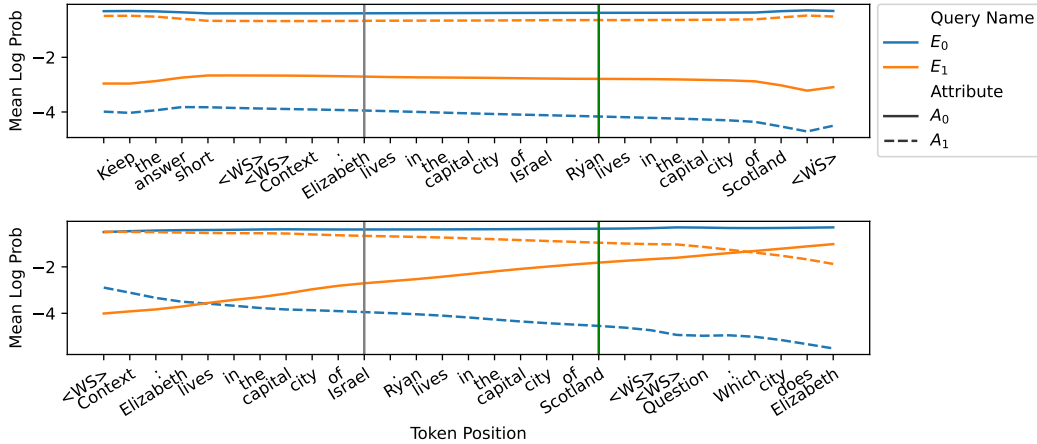


Figure 4: Top: Mean log probs for entity interventions. Bottom: Mean log probs for attributes. For brevity, let Z_k refer to Z_{E_k} or Z_{A_k} . The grey and green vertical lines indicate the original positions for Z_0 and Z_1 respectively. The x-axis marks x , Z_0 's new position. Under the position interventions $\{X_0 \rightarrow x, X_1 \rightarrow X_1 - (x - X_0)\}$, the grey line is the *control condition* with no interventions, and the green line is the *swapped condition* where Z_0 and Z_1 have swapped positions.

Results are shown in Fig. 3 and support the factorizability hypothesis. As an example, consider Fig. 3a. In the None setting (no intervention), we see high log probs for A_0 when queried for E_0 , and for A_1 when queried for E_1 . This indicates that the LM is able to solve this task. Next, consider the Attribute intervention setting ($A_0 \rightarrow A'_0$): querying for E_0 now gives high log probs for A'_0 , and querying for E_1 gives A_1 as usual. Finally, in the Both setting (where both entity and attribute are swapped), querying E'_0 returns A'_0 while querying E_0 leads to approximately uniform predictions.

Experiment details. We use LLaMA 30-b here and elsewhere unless otherwise stated. In practice, we found that activations for both the entity token and the subsequent token encode the entity binding information. Thus for all experiments in this paper, we expand the definition of Z_{E_k} to include the token activations immediately after E_k .

3.2 POSITION INDEPENDENCE

We next turn to position independence, which is the other property we expect LMs implementing the binding ID mechanism to have. This says that permuting the order of the Z_{E_k} and Z_{A_k} should

have no effect on the output, because the LM looks only at the binding IDs and not the positions of entities or attributes activations.

To apply causal interventions to the positions, we use the fact that transformers use positional embeddings to encode the (relative) position of each token in the input. We can thus intervene on these embeddings to “move” one of the Z_k ’s to another location k' . Formally, we let X_k describe the position embedding for Z_k , and denote the position intervention as $\{X_k \rightarrow k'\}$. In Appendix C we describe how to do this for rotary position embeddings (RoPE), which underlie all the models we study. For now, we will assume this intervention as a primitive and discuss experimental results.

For our experiments, we again consider the CAPITALS task with $n = 2$. Let X_{E_0} and X_{E_1} denote the positions of the two entities. We apply interventions of the form $\{X_{E_0} \rightarrow x, X_{E_1} \rightarrow X_{E_1} - (x - X_{E_0})\}$, for $x \in \{X_{E_0}, X_{E_0} + 1, \dots, X_{E_1}\}$. This measures the effect of gradually moving the two entity positions past each other: when $x = X_{E_0}$, no intervention is performed (*control condition*), and when $x = X_{E_1}$ the entity positions are swapped (*swapped condition*). We repeat the same experiment with attribute activations and measure the mean log probs in both cases.

Results are shown in Fig. 4. As predicted under position independence, position interventions result in little change in model behavior. Consider the *swapped condition* at the green line. Had the binding information been entirely encoded in position, we expect a complete switch in beliefs compared to the *control condition*. In reality, we observe almost no change in mean log probs for entities and a small change in mean log probs for attributes that seems to be part of an overall gradual trend.

We interpret this gradual trend as an artifact of *position-dependent bias*, and not as evidence against position independence. We view it as a bias because it affects all attributes regardless of how they are bound—attributes that are shifted to later positions always have higher log probs. We provide further discussion of this bias, as well as other experimental details, in Appendix C.

4 STRUCTURE OF BINDING ID

The earlier section shows evidence for the binding ID mechanism. Here, we investigate two hypotheses on the structure of binding IDs and binding functions. The first is that the binding functions Γ_A and Γ_E are additive, which lets us think of binding IDs as *binding vectors*. The second is contingent on the first, and asks if binding vectors have a geometric relationship between each other.

4.1 ADDITIVITY OF BINDING FUNCTIONS

Prior interpretability research has proposed that transformers represent features linearly (Elhage et al., 2021). Therefore a natural hypothesis is that both entity/attribute representations and abstract binding IDs are vectors in activation space, and that the binding function simply adds the vectors for entity/attribute and binding ID. We let the binding ID k be represented by the pair of vectors $[b_E(k), b_A(k)]$, and the representations of entity e and attribute a be $f_E(e)$ and $f_A(a)$ respectively. Then, we hypothesize that the binding functions can be linearly decomposed as:

$$\Gamma_A(a, k) = f_A(a) + b_A(k), \quad \Gamma_E(e, k) = f_E(e) + b_E(k). \quad (1)$$

Binding ID vectors seem intuitive and plausibly implementable by transformer circuits. To experimentally test this, we seek to extract $b_A(k)$ and $b_E(k)$ in order to perform vector arithmetic on them. We use (1) to extract the *differences* $\Delta_E(k) := b_E(k) - b_E(0)$, $\Delta_A(k) := b_A(k) - b_A(0)$. Rearranging (1), we obtain

$$\Delta_A(k) = \Gamma_A(\alpha, k) - \Gamma_A(\alpha, 0), \quad \Delta_E(k) = \Gamma_E(a, k) - \Gamma_E(a, 0). \quad (2)$$

We estimate $\Delta_A(k)$ by sampling $\mathbb{E}_{\mathbf{c}, \mathbf{c}'}[Z_{A_k}(\mathbf{c}) - Z_{A_0}(\mathbf{c}')]$, and likewise for $\Delta_E(k)$.

Mean interventions. With the difference vectors, we can modify binding IDs by performing *mean interventions*, and observe how model behavior changes. The attribute mean intervention switches the binding ID vectors in Z_{A_0} and Z_{A_1} with the interventions $Z_{A_0} \rightarrow Z_{A_0} + \Delta_A(1)$, $Z_{A_1} \rightarrow Z_{A_1} - \Delta_A(1)$. The entity mean intervention similarly switches the binding ID vectors in Z_{E_0} and Z_{E_1} . Additivity predicts that performing either mean intervention will reverse the model behavior: E_0 will be associated with A_1 , and E_1 with A_0 .

Test condition	Control	Attribute	Entity	Both	Attribute	Entity	Both
Querying E_0	0.99	0.00	0.00	0.97	0.98	0.98	0.97
Querying E_1	1.00	0.03	0.01	0.99	1.00	1.00	1.00

Table 1: Left: Mean calibrated accuracies for mean interventions on four test conditions. Columns are the test conditions, and rows are queries. Right: Mean interventions with random vectors.

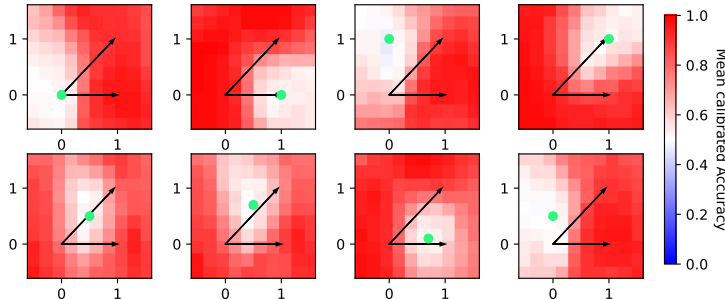


Figure 5: The plots show the mean median-calibrated accuracy when one pair of binding ID, v_0 , is fixed at the green circle, and the other, v_1 , is varied across the grid. The binding IDs $b(0)$, $b(1)$, and $b(2)$ are shown as the origin of the arrows, the end of the horizontal arrow, and the end of the diagonal arrow respectively. We use LLaMA-13b for computational reasons.

Experiments. In our experiments, we fix $n = 2$ and use 500 samples to estimate $\Delta_E(1)$ and $\Delta_A(1)$. We then perform four tests, and evaluate the model accuracy under the original belief. The Control test has no interventions, and the accuracy reflects model’s base performance. The Attribute and Entity tests perform the attribute and entity mean interventions, which should lead to a complete switch in model beliefs so that the accuracy is near 0. Table 1 shows agreement with additivity: the accuracies are above 99% for Control, and below 3% for Attribute and Entity.

As a further check, we perform both attribute and entity mean interventions simultaneously, which should cancel out and thus restore accuracy. Indeed, Table 1 shows that accuracy for Both is above 97%. Finally, to show that the *specific* directions obtained by the difference vectors matter, we sample random vectors with the same magnitude but random directions, and perform the same mean interventions with the random vectors. These random vectors have no effect on the model behavior.

4.2 THE GEOMETRY OF BINDING ID VECTORS

Section 4.1 shows that we can think of binding IDs as pairs of ID vectors, and that randomly chosen vectors do not function as binding IDs. We next investigate the geometric structure of valid binding vectors and find that linear interpolations or extrapolations of binding vectors are often also valid binding vectors. This suggests that binding vectors occupy a continuous *binding subspace*. We find evidence of a metric structure in this space, such that nearby binding vectors are hard for the model to distinguish, but far-away vectors can be reliably distinguished and thus used for the binding task.

To perform our investigation, we apply variants of the mean interventions in Section 4.1. As before, we start with an $n = 2$ context, thus obtaining representations $Z_0 = (Z_{E_0}, Z_{A_0})$ and $Z_1 = (Z_{E_1}, Z_{A_1})$. We first erase the binding information by subtracting $(\Delta_E(1), \Delta_A(1))$ from Z_1 , which reduces accuracy to chance. Next, we will add vectors $v_0 = (v_{E_0}, v_{A_0})$ and $v_1 = (v_{E_1}, v_{A_1})$ to the representations Z ; if doing so restores accuracy, then we view (v_{E_0}, v_{A_0}) and (v_{E_1}, v_{A_1}) as valid binding pairs.

To generate different choices of v , we take linear combinations across a two-dimensional space. The basis vectors for this space are $(\Delta_E(1), \Delta_A(1))$ and $(\Delta_E(2), \Delta_A(2))$ obtained by averaging across an $n = 3$ context. Fig. 5 shows the result for several different combinations, where the coordinates of v_0 are fixed and shown in green while the coordinates of v_1 vary. When v_1 is close to v_0 , the LM gets close to 50% accuracy, which indicates confusion. Far away from v_1 , the network consistently achieves high accuracy, demonstrating that linear combinations of binding IDs (even with negative coefficients) are themselves valid binding IDs. See Appendix G for details.

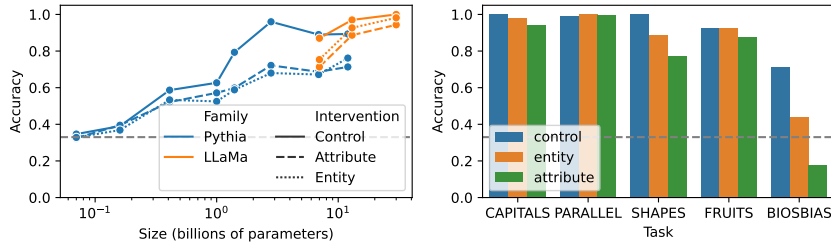


Figure 6: Left: models in Pythia and LLaMA on CAPITALS. LLaMA-65b not present for computational reasons. Right: LLaMA-30b on binding tasks. Unlike others, the BIOS task has attributes that are several tokens long.

Task	CAPITALS	PARALLEL	SHAPES	FRUITS	BIOS	Zeros	Random
Mean accuracy	0.88	0.87	0.71	0.80	0.47	0.30	0.31
Mean log prob	-1.01	-1.07	-1.18	-1.21	-1.64	-1.86	-2.15

Table 2: The mean median-calibrated accuracy and mean log prob for mean interventions on $n = 3$ CAPITALS using binding ID estimates from other tasks. Random chance has 0.33 mean accuracy.

The geometry of the binding subspace hints at circuits (Elhage et al., 2021) in LMs that process binding vectors. For example, we speculate that certain attention heads might be responsible for comparing binding ID vectors, since the attention mechanism computes attention scores using a quadratic form which could provide the metric over the binding subspace.

5 GENERALITY AND LIMITATIONS OF BINDING ID

The earlier sections investigate binding IDs for one particular task: the CAPITALS task. In this section, we evaluate their generality. We first show that binding vectors are used for a variety of tasks and models. We then show evidence that the binding vectors are task-agnostic: vectors from one task transfer across many different tasks. However, we show that our mechanism is not fully universal, by exhibiting a question-answering task that uses an alternative binding mechanism.

Generality of binding ID vectors. We evaluate the generality of binding vectors across models and tasks. For a (model, task) pair, we compute the median-calibrated accuracy on the $n = 3$ context under three conditions: (1) the control condition in which no interventions are performed, and the (2) entity and (3) attribute conditions in which entity or attribute mean interventions (Section 4.1) are performed. We use the mean interventions to permute binding pairs by a cyclic shift and measure accuracy according to this shift (see Appendix F). As shown in Figure 6, the interventions induce the expected behavior on most tasks; moreover, their effectiveness increases with model scale, suggesting that larger models have more robust structured representations.

Transfer across tasks. We next show that binding vectors often transfer across tasks. Without access to the binding vectors $[b_E(k), b_A(k)]$, we instead test if the difference vectors $[\Delta_E^{\text{src}}(k), \Delta_A^{\text{src}}(k)]$ from a source task, when applied to a target task, result in valid binding IDs. To do so, we follow a similar procedure to Section 4.2: First, we erase binding information by subtracting $[\Delta_E^{\text{tar}}(k), \Delta_A^{\text{tar}}(k)]$ for the target task from each target-task representation $[Z_{E_k}, Z_{A_k}]$, which results in near-chance accuracy. Then, we add back in $[\Delta_E^{\text{src}}(k), \Delta_A^{\text{src}}(k)]$ computed from the source task with the hope of restoring performance.

Table 2 shows results for a variety of source tasks when using CAPITALS as the target task. Accuracy is consistently high, even when the target task has limited surface similarity to the target task. For example, the SHAPES task contains descriptions about geometrical shapes and their colors, and PARALLEL puts all entities before any attributes instead of interleaving them as in CAPITALS. We include two baselines for comparison: replacing $\Delta^{\text{src}}(k)$ with the zero vector (“Zeros”), or picking a randomly oriented difference vector as in Table 1 (“Random”). Both lead to chance accuracy. See Appendix D for more details on the tasks.

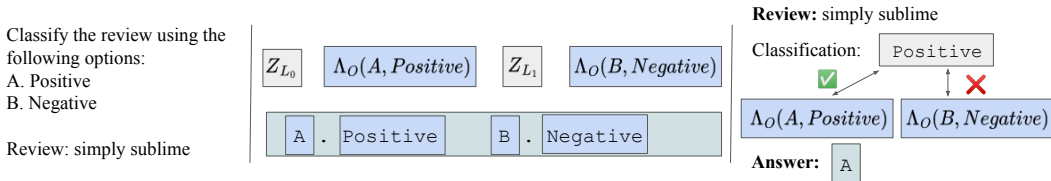


Figure 7: Direct binding in MCQ task. O_k and L_k denote options and labels respectively. Under direct binding, Z_{O_0} and Z_{O_1} are represented by a binding function Λ_O that directly binds option and label together, whereas Z_{L_0} and Z_{L_1} are causally irrelevant.

The fact that binding vectors transfer across tasks, together with the results from Section 4, suggests that there could be a task-agnostic subspace in the model’s activations reserved for binding vectors.

Direct binding in MCQ. While binding IDs are used for many tasks, they are not universal. We briefly identify an alternate binding mechanism, the *direct binding* mechanism, that is used for a multiple-choice question-answering task (MCQ). In MCQ, each label (A or B) has to be bound to its associated option text. In this task, instead of binding variables to an abstract binding ID, the model directly binds the label to the option (Fig. 7). We provide the full details of this task and further explanations in Appendix E.

6 RELATED WORK

Causal mediation analysis. In recent years, causal methods have gained popularity in post hoc interpretability (Meng et al., 2022; Geiger et al., 2021). Instead of relying on correlations, which could lead to spurious features (Hewitt & Liang, 2019), causal mediation analysis (Vig et al., 2020a) performs causal interventions on internal states of LMs to understand their causal role on LM behavior. Our work shares the same causal perspective adopted by many in this field.

Knowledge recall. A line of work studies recalling factual associations that LMs learn from pre-training (Geva et al., 2020; Dai et al., 2021; Meng et al., 2022; Geva et al., 2023; Hernandez et al., 2023b). This is spiritually related to binding, as entities must be associated to facts about them. However, this work studies factual relations learned from *pretraining* and how they are recalled from model *weights*. In contrast, we study representations of relations learned from *context*, and how they are recalled from model *activations*.

More recently, Hernandez et al. (2023a) found a method to construct bound representations by directly binding attribute representations to entity representations. In contrast, our work investigates bound representations constructed by the LM itself, and identifies that the binding ID mechanism (and not direct binding) is the mechanism that LM representations predominantly uses. An avenue for future work is to study how bound representations constructed by Hernandez et al. (2023a) relates to the direct binding mechanism we identified in the MCQ task.

Symbolic representations in connectionist systems. Many works have studied how neural networks represent symbolic concepts in activation space (Mikolov et al., 2013; Tenney et al., 2019; Belinkov & Glass, 2019; Rogers et al., 2021; Patel & Pavlick, 2021). To gain deeper insights into how these representations are used for reasoning, recent works have studied representations used for specialized reasoning tasks (Nanda et al., 2023; Li et al., 2022; 2021). Our work shares the motivation of uncovering how neural networks implement structured representations that enable reasoning.

Mechanistic Interpretability. Mechanistic interpretability aims to uncover circuits (Elhage et al., 2021; Wang et al., 2022; Wu et al., 2023), often composed of attention heads, that are embedded in language models. In our work, we study language model internals on a more coarse-grained level. We identify structures in representations that have causal influences on model behavior, but how circuits construct these representations or utilize them is left as future work.

7 CONCLUSION

In this paper we identify and study the binding problem, a common and fundamental reasoning subproblem. We find that pretrained LMs can solve the binding task by binding entities and attributes to abstract binding IDs. Then, we identify that the binding IDs are vectors from a binding subspace with a notion of distance. Lastly, we find that the binding IDs are used broadly for a variety of binding tasks and are present in all sufficiently large models that we studied.

Taking a broader view, we see our work as a part of the endeavor to interpret LM reasoning by decomposing it into primitive skills. In this work we identified the binding skill, which is used in several settings and has a simple and robust representation structure. An interesting direction of future work would be to identify other primitive skills that support general purpose reasoning and have similarly interpretable mechanisms.

Our work also suggests that ever-larger LMs may still have interpretable representations. A common intuition is that larger models are more complex, and hence more challenging to interpret. Our work provides a counterexample: as LMs become larger, their representations can become *more* structured and interpretable, since only the larger models exhibited binding IDs (Fig. 6).

Speculating further, the fact that large enough models in two unrelated LM families learn the same structured representation strategy points to a convergence in representations with scale. This raises the philosophical question: could there be an ultimate representation that these LMs are converging towards? Perhaps the properties of natural language corpora and LM inductive biases lead to the inevitable development of certain core representation strategies that are invariant to changes in model hyperparameters or exact dataset composition. This would encouragingly imply that interpretability results can transfer across models—studying the core representations of any sufficiently large model would yield insights into other similarly large models because of their convergent core structure.

ACKNOWLEDGMENTS

We thank Danny Halawi, Fred Zhang, Erik Jenner, Cassidy Laidlaw, Shawn Im, Arthur Conmy, Shivam Singhal, and Olivia Watkins for their helpful feedback. JF was supported by the Long-Term Future Fund. JS was supported by the National Science Foundation under Grants No. 2031899 and 1804794. In addition, we thank Open Philanthropy for its support of both JS and the Center for Human-Compatible AI.

REFERENCES

- Yonatan Belinkov and James Glass. Analysis methods in neural language processing: A survey. *Transactions of the Association for Computational Linguistics*, 7:49–72, 2019. doi: 10.1162/tacl.a.00254. URL <https://aclanthology.org/Q19-1004>.
- Stella Biderman, Hailey Schoelkopf, Quentin Gregory Anthony, Herbie Bradley, Kyle O’Brien, Eric Hallahan, Mohammad Aflah Khan, Shivanshu Purohit, USVSN Sai Prashanth, Edward Raff, et al. Pythia: A suite for analyzing large language models across training and scaling. In *International Conference on Machine Learning*, pp. 2397–2430. PMLR, 2023.
- Damai Dai, Li Dong, Yaru Hao, Zhifang Sui, and Furu Wei. Knowledge neurons in pretrained transformers. *ArXiv*, abs/2104.08696, 2021. URL <https://api.semanticscholar.org/CorpusID:233296761>.
- Maria De-Arteaga, Alexey Romanov, Hanna Wallach, Jennifer Chayes, Christian Borgs, Alexandra Chouldechova, Sahin Geyik, Krishnaram Kenthapadi, and Adam Tauman Kalai. Bias in bios: A case study of semantic representation bias in a high-stakes setting. In *proceedings of the Conference on Fairness, Accountability, and Transparency*, pp. 120–128, 2019.
- Nelson Elhage, Neel Nanda, Catherine Olsson, Tom Henighan, Nicholas Joseph, Ben Mann, Amanda Askell, Yuntao Bai, Anna Chen, Tom Conerly, Nova DasSarma, Dawn Drain, Deep Ganguli, Zac Hatfield-Dodds, Danny Hernandez, Andy Jones, Jackson Kernion, Liane Lovitt, Kamal Ndousse, Dario Amodei, Tom Brown, Jack Clark, Jared Kaplan, Sam McCandlish, and Chris Olah. A mathematical framework for transformer circuits. *Transformer Circuits Thread*, 2021. <https://transformer-circuits.pub/2021/framework/index.html>.

- Atticus Geiger, Hanson Lu, Thomas Icard, and Christopher Potts. Causal abstractions of neural networks. *Advances in Neural Information Processing Systems*, 34:9574–9586, 2021.
- Mor Geva, R. Schuster, Jonathan Berant, and Omer Levy. Transformer feed-forward layers are key-value memories. *ArXiv*, abs/2012.14913, 2020. URL <https://api.semanticscholar.org/CorpusID:229923720>.
- Mor Geva, Jasmijn Bastings, Katja Filippova, and Amir Globerson. Dissecting recall of factual associations in auto-regressive language models. *arXiv preprint arXiv:2304.14767*, 2023.
- Dan Hendrycks, Nicholas Carlini, John Schulman, and Jacob Steinhardt. Unsolved problems in ml safety. *arXiv preprint arXiv:2109.13916*, 2021.
- Evan Hernandez, Sarah Schwettmann, David Bau, Teona Bagashvili, Antonio Torralba, and Jacob Andreas. Natural language descriptions of deep visual features. In *International Conference on Learning Representations*, 2021.
- Evan Hernandez, Belinda Z Li, and Jacob Andreas. Measuring and manipulating knowledge representations in language models. *arXiv preprint arXiv:2304.00740*, 2023a.
- Evan Hernandez, Arnab Sen Sharma, Tal Haklay, Kevin Meng, Martin Wattenberg, Jacob Andreas, Yonatan Belinkov, and David Bau. Linearity of relation decoding in transformer language models. *arXiv preprint arXiv:2308.09124*, 2023b.
- John Hewitt and Percy Liang. Designing and interpreting probes with control tasks. *arXiv preprint arXiv:1909.03368*, 2019.
- Belinda Z Li, Maxwell Nye, and Jacob Andreas. Implicit representations of meaning in neural language models. *arXiv preprint arXiv:2106.00737*, 2021.
- Kenneth Li, Aspen K Hopkins, David Bau, Fernanda Viégas, Hanspeter Pfister, and Martin Wattenberg. Emergent world representations: Exploring a sequence model trained on a synthetic task. *arXiv preprint arXiv:2210.13382*, 2022.
- Kevin Meng, David Bau, Alex Andonian, and Yonatan Belinkov. Locating and editing factual associations in gpt. *Advances in Neural Information Processing Systems*, 35:17359–17372, 2022.
- Tomáš Mikolov, Wen-tau Yih, and Geoffrey Zweig. Linguistic regularities in continuous space word representations. In *Proceedings of the 2013 conference of the north american chapter of the association for computational linguistics: Human language technologies*, pp. 746–751, 2013.
- Jesse Mu and Jacob Andreas. Compositional explanations of neurons. *Advances in Neural Information Processing Systems*, 33:17153–17163, 2020.
- Neel Nanda, Lawrence Chan, Tom Lieberum, Jess Smith, and Jacob Steinhardt. Progress measures for grokking via mechanistic interpretability. In *The Eleventh International Conference on Learning Representations*, 2023. URL <https://openreview.net/forum?id=9XFSbDPmdW>.
- Roma Patel and Ellie Pavlick. Mapping language models to grounded conceptual spaces. In *International Conference on Learning Representations*, 2021.
- Tilman Räuher, Anson Ho, Stephen Casper, and Dylan Hadfield-Menell. Toward transparent ai: A survey on interpreting the inner structures of deep neural networks. In *2023 IEEE Conference on Secure and Trustworthy Machine Learning (SaTML)*, pp. 464–483. IEEE, 2023.
- Anna Rogers, Olga Kovaleva, and Anna Rumshisky. A primer in bertology: What we know about how bert works. *Transactions of the Association for Computational Linguistics*, 8:842–866, 2021.
- Richard Socher, Alex Perelygin, Jean Wu, Jason Chuang, Christopher D. Manning, Andrew Ng, and Christopher Potts. Recursive deep models for semantic compositionality over a sentiment treebank. In *Proceedings of the 2013 Conference on Empirical Methods in Natural Language Processing*, pp. 1631–1642, Seattle, Washington, USA, October 2013. Association for Computational Linguistics. URL <https://www.aclweb.org/anthology/D13-1170>.

- Jianlin Su, Yu Lu, Shengfeng Pan, Ahmed Murtadha, Bo Wen, and Yunfeng Liu. Roformer: Enhanced transformer with rotary position embedding. *arXiv preprint arXiv:2104.09864*, 2021.
- Ian Tenney, Dipanjan Das, and Ellie Pavlick. Bert rediscovers the classical nlp pipeline. In *Association for Computational Linguistics*, 2019. URL <https://arxiv.org/abs/1905.05950>.
- Hugo Touvron, Thibaut Lavril, Gautier Izacard, Xavier Martinet, Marie-Anne Lachaux, Timothée Lacroix, Baptiste Rozière, Naman Goyal, Eric Hambro, Faisal Azhar, et al. Llama: Open and efficient foundation language models. *arXiv preprint arXiv:2302.13971*, 2023.
- Anne Treisman. The binding problem. *Current opinion in neurobiology*, 6(2):171–178, 1996.
- Jesse Vig, Sebastian Gehrmann, Yonatan Belinkov, Sharon Qian, Daniel Nevo, Yaron Singer, and Stuart Shieber. Investigating gender bias in language models using causal mediation analysis. *Advances in neural information processing systems*, 33:12388–12401, 2020a.
- Jesse Vig, Sebastian Gehrmann, Yonatan Belinkov, Sharon Qian, Daniel Nevo, Yaron Singer, and Stuart Shieber. Investigating gender bias in language models using causal mediation analysis. *Advances in Neural Information Processing Systems*, 33:12388–12401, 2020b.
- Kevin Wang, Alexandre Variengien, Arthur Conmy, Buck Shlegeris, and Jacob Steinhardt. Interpretability in the wild: A circuit for indirect object identification in gpt-2 small. *arXiv preprint arXiv:2211.00593*, 2022.
- Yizhong Wang, Hamish Ivison, Pradeep Dasigi, Jack Hessel, Tushar Khot, Khyathi Raghavi Chandu, David Wadden, Kelsey MacMillan, Noah A Smith, Iz Beltagy, et al. How far can camels go? exploring the state of instruction tuning on open resources. *arXiv preprint arXiv:2306.04751*, 2023.
- Zhengxuan Wu, Atticus Geiger, Christopher Potts, and Noah D Goodman. Interpretability at scale: Identifying causal mechanisms in alpaca. *arXiv preprint arXiv:2305.08809*, 2023.
- Zihao Zhao, Eric Wallace, Shi Feng, Dan Klein, and Sameer Singh. Calibrate before use: Improving few-shot performance of language models. In *International Conference on Machine Learning*, pp. 12697–12706. PMLR, 2021.

A EVALUATION DETAILS

In all of our evaluations, we sample $N = 100$ instances of contexts from the binding task, obtaining $\{\mathbf{c}_i\}_{i=1}^N$. For succinctness, we write $E_k^{(i)} := E_k(\mathbf{c}_i)$ and $A_k^{(i)} := A_k(\mathbf{c}_i)$. For the i -th context instance, we query $E_0^{(i)}$ and $E_1^{(i)}$ which return log probabilities $\Phi_{E_0}^{(i)}(t)$ and $\Phi_{E_1}^{(i)}(t)$ over tokens t in the vocabulary. However, we consider only the log probabilities for relevant attributes $\Phi_{E_k}^{(i)}(A_0^{(i)})$ and $\Phi_{E_k}^{(i)}(A_1^{(i)})$. We then compute the summary statistics (described below) over the entire population of samples so that we get two scalars, σ_{E_0} and σ_{E_1} describing the performance under each query entity.

- The **mean log prob** is given by $\sigma_{E_k} = \frac{1}{N} \sum_{i=1}^N \Phi_{E_k}^{(i)}(A_k^{(i)})$.
- The **top-1 accuracy** is $\sigma_{E_k} = \frac{1}{N} \sum_{i=1}^N \mathbf{1}[k = \arg \max_l \Phi_{E_k}^{(i)}(A_l^{(i)})]$.
- We adopt the **median calibrated accuracy** from [Zhao et al. \(2021\)](#). First, we obtain a baseline by computing medians for every attribute $m(A_l) := \text{median}_{i,k} \{\Phi_{E_k}^{(i)}(A_l^{(i)})\}$. Then, compute calibrated log probs $\tilde{\Phi}_{E_k}^{(i)}(A_l) := \Phi_{E_k}^{(i)}(A_l) - m(A_l)$. The median calibrated accuracy is then $\sigma_{E_k} = \frac{1}{N} \sum_{i=1}^N \mathbf{1}[k = \arg \max_l \tilde{\Phi}_{E_k}^{(i)}(A_l^{(i)})]$.

[Zhao et al. \(2021\)](#) discusses motivations for the median calibrated accuracy. In our case, the position dependent bias provides additional reasons, which we discuss in Appendix C.

B NECESSITY OF BINDING ID MECHANISM

In this section, we provide one definition of the binding ID mechanism, and argue informally that under this definition, factorizability and position independence necessarily implies the binding ID mechanism.

First, let us define the binding ID mechanism. Fix $n = 2$ for simplicity. There are two claims:

1. **Representation.** There exists a binding function Γ_E such that for any contexts \mathbf{c} , Z_{E_k} is represented by $\Gamma_E(E_k, k)$, in the sense that for any $e \in \mathcal{E}$, $\{Z_{E_k} \rightarrow \Gamma_E(e, k)\}$ leads to the belief $\mathbf{c}/.\{E_k \rightarrow e\}$. Likewise, there exists a binding function Γ_A such that for any contexts \mathbf{c} , Z_{A_k} is represented by $\Gamma_A(A_k, k)$, in the sense that for any $a \in \mathcal{A}$, $\{Z_{A_k} \rightarrow \Gamma_A(a, k)\}$ leads to the belief $\mathbf{c}/.\{A_k \rightarrow a\}$. These substitutions should also compose appropriately.
2. **Query.** Further, the binding functions Γ_A and Γ_E satisfy the following property: Choose any 2 permutations $\pi_E(k)$ and $\pi_A(k)$ over $\{0, 1\}$, and consider a Z_{context} containing $[\Gamma_E(e_0, \pi_E(0)), \Gamma_A(a_0, \pi_A(0)), \Gamma_E(e_1, \pi_E(1)), \Gamma_A(a_1, \pi_A(1))]$. The query system will then believe $e_0 \leftrightarrow a_0, e_1 \leftrightarrow a_1$ if $\pi_E = \pi_A$, and $e_0 \leftrightarrow a_1, e_1 \leftrightarrow a_0$ otherwise.

The first claim follows from factorizability. From factorizability, we can construct the candidate binding functions simply by picking an arbitrary context consistent with the parameters. For any $e \in \mathcal{E}$ and any binding ID $k \in [0, n - 1]$, pick any context \mathbf{c} such that $E_k(\mathbf{c}) = e$. Then, let $\Gamma_E(e, k) = Z_{E_k}(\mathbf{c})$. Γ_A can be constructed similarly. Our factorizability results show that the binding functions constructed this way satisfy the **Representation** claim.

The second claim follows from **Representation** and position independence. Pick an arbitrary context \mathbf{c} to generate Z_{context} . Then, by factorizability we can make the substitutions $Z_{E_k} \rightarrow \Gamma_E(e_{\pi_E^{-1}(k)}, k)$ and $Z_{A_k} \rightarrow \Gamma_A(a_{\pi_A^{-1}(k)}, k)$, to obtain

$$[\Gamma_E(e_{\pi_E^{-1}(0)}, 0), \Gamma_A(a_{\pi_A^{-1}(0)}, 0), \Gamma_E(e_{\pi_E^{-1}(1)}, 1), \Gamma_A(a_{\pi_A^{-1}(1)}, 1)].$$

Because of factorizability, the model believes $e_0 \leftrightarrow a_0, e_1 \leftrightarrow a_1$ if $\pi_E = \pi_A$, and $e_0 \leftrightarrow a_1, e_1 \leftrightarrow a_0$ otherwise. Now, position independence lets us freely permute $\{Z_{E_0}, Z_{E_1}\}$ and $\{Z_{A_0}, Z_{A_1}\}$ without changing beliefs, which achieves the desired

$$[\Gamma_E(e_0, \pi_E(0)), \Gamma_A(a_0, \pi_A(0)), \Gamma_E(e_1, \pi_E(1)), \Gamma_A(a_1, \pi_A(1))].$$

C DETAILS FOR POSITION INDEPENDENCE

RoPE Intervention. In Fig. 2a, the context activations Z_{context} is drawn in a line, suggesting a linear form: $Z_{\text{context}} = [\dots, Z_{E_0}, \dots, Z_{A_0}, \dots, Z_{E_1}, \dots, Z_{A_1}, \dots]$. We can equivalently think of Z_{context} as a set of pairs: $Z_{\text{context}} = \{(p, Z_p) \mid p \text{ is an index for a context token}\}$. LMs that use Rotary Position Embedding (RoPE) (Su et al., 2021), such as those in the LLaMA and Pythia families, have architectures that allow arbitrarily intervention on the apparent position of an activation $(p, Z_p) \rightarrow (p', Z_p)$, even if this results in overall context activations that cannot be written down as a list of activations. This is because position information is applied at every layer, and not injected into the residual stream like in absolute position embeddings. Specifically, equation 16 in Su et al. (2021) provides the definition of RoPE (recreated verbatim as follows):

$$q_m^\top k_n = (\mathbf{R}_{\Theta, m}^d \mathbf{W}_q x_m)^\top (\mathbf{R}_{\Theta, n}^d \mathbf{W}_k x_n) \quad (3)$$

Then, making the intervention $\mathbf{R}_{\Theta, n}^d \rightarrow \mathbf{R}_{\Theta, n^*}^d$ changes the apparent position of the activations at position n to the position at n^* .

Is the position dependent bias just a bias? For the purposes of determining if *position* encodes *binding*, the fact that the LM does not substantially change its beliefs when we switch the positions of the attribute activations (or the entity activations) suggests that position can only play a limited role. However, calling the position dependency of attributes a ‘‘bias’’ implies that it is an artifact that we should correct for. To what extent is this true?

The case for regarding it as a bias is two-fold. First, as discussed by Su et al. (2021), RoPE exhibits long-term position decay, which systematically lowers the attention paid to activations that are further away from the query (i.e. earlier in the context). Plausibly, at some point when computing

the query mechanism, the LM has to make a decision whether to pay attention to the first or the second attribute, and the presence of the long-term position decay can bias this decision, leading to the position dependent bias in the final prediction that we see.

The second reason is that there are systematic and unbiased ways of calibrating the LM to recover the correct answer, in spite of the position dependent bias. We discuss two strategies. Because the position dependent bias modifies the log probs for A_0 (or A_1) regardless of which entity is being queried, we can estimate this effect by averaging the log probs for A_0 (or A_1) for both queries E_0 and E_1 . Then, when making a prediction, we can subtract this average from the log probs for A_0 (or A_1). This corresponds to the *median calibrated accuracy* metric discussed earlier. The second procedure to mitigate the position dependent bias is an intervention to set all attribute activations to have the same position, which limits the amount of bias position dependency can introduce.

These procedures do not require foreknowledge of what the ground truth predicates are, and hence do not leak knowledge into the prediction process — if the calibrated LM answers queries correctly, the information must have come from the context activations and not from the calibration process.

Nonetheless, there are features about the position dependent bias that could be interesting to study. For example, we might hope to predict the magnitudes of the position dependent bias based on RoPE’s parameters. However, such an investigation will most likely involve a deeper mechanistic understanding of the query system, which we leave as future work.

D BINDING TASK DETAILS

D.1 CAPITALS

Construct a list of one-token names and a list of country-capital pairs that are also each one-token wide. Then, apply the following template:

Answer the question based on the context below. Keep the answer short.

Context: {E_0} lives in the capital city of {A_0}.
{E_1} lives in the capital city of {A_1}.

Question: Which city does {qn_subject} live in?

Answer: {qn_subject} lives in the city of

The LM is expected to answer with the capital of the country that is bound to the queried entity. Note that the LM is expected to simultaneously solve the factual recall task of looking up the capital city of a country.

D.2 PARALLEL

The PARALLEL task uses the same country capital setup, but with the prompt template:

Answer the question based on the context below. Keep the answer short.

Context: {E_0} and {E_1} live in the capital cities of {A_0} and {A_1} respectively.

Question: Which city does {qn_subject} live in?

Answer: {qn_subject} lives in the city of

This prompt format breaks the confounder in the CAPITALS task that entity always appear in the same sentence as attributes, suggesting binding ID is not merely a syntactic property.

D.3 FRUITS

The FRUITS task uses the same set of names, but for attributes it uses a set of common fruits and food that are one-token wide. The prompt format is:

Answer the question based on the context below. Keep the answer short.

Context: {E_0} likes eating the {A_0}. {E_1} likes eating the {A_1} respectively.

Question: What food does {qn_subject} like?

Answer: {qn_subject} likes the

D.4 SHAPES

The SHAPES tasks have entities which are one-token wide *colors*, and attributes which are one-token wide *shapes*. The prompt looks like:

Answer the question based on the context below. Keep the answer short.

Context: The {A_0} is {E_0}. The {A_1} is {E_1}.

Question: Which shape is colored {qn_subject}?

Answer: The {qn_subject} shape is

This task inverts the assumption that entities have to be nouns, and attributes are adjectives.

D.5 BIOS

This task is adapted from the bias in bios dataset [De-Arteaga et al. \(2019\)](#), with a prompt format following [Hernandez et al. \(2023a\)](#). The entities are the set of one-token names, and the attributes are a set of biography descriptions obtained using the procedure from [Hernandez et al. \(2023a\)](#). The LM is expected to infer the occupation from this description. This time, the attributes are typically one sentence long, and are no longer one-token wide. We thus do not expect the mean interventions for attributes to work, although we may still expect entity interventions to work. Just inferring the correct occupation is also a much more challenging task than the other synthetic tasks.

The prompt format is:

Answer the question based on the context below. Keep the answer short.

Context:
About {E_0}: {A_0}
About {E_1}: {A_1}

Question: What occupation does {qn_subject} have?

Answer: {qn_subject} has the occupation of

E MCQ TASK

Multiple choice questions (MCQs) can be formulated as a binding task if we put the options *before* the question. This is to force the LM to represent the binding between label and option text before it sees the questions. We study the SST-2 task ([Socher et al., 2013](#)), which is a binary sentiment classification task on movie reviews (either positive or negative). Then, the attributes are single letter labels from A to E, and the entities are “Positive” and “Negative”.

The prompt is as follows:

Classify the review using the following options:
{A_0}: {E_0}
{A_1}: {E_1}
Review: {question}
Answer:

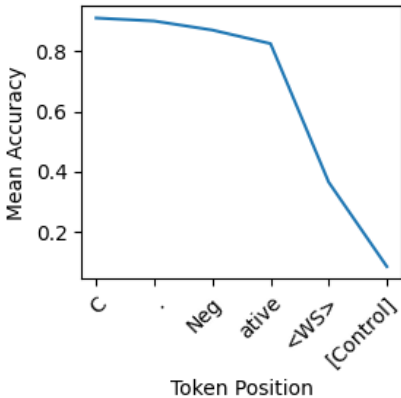


Figure 8: Substitutions for MCQ option suffix

Then, when prompted with a question with a certain sentiment, the LM is expected to retrieve its corresponding label.

E.1 EXPERIMENTS

It turns out that the reversed MCQ format is too out of distribution for LLaMA-30b to solve. However, we find that the instruction finetuned tulu-13b model (Wang et al., 2023) is able to solve this task.

We find that the activations for this task are not factorizable in the same way. Consider the target context:

```
C: Negative
A: Positive
```

and the source context:

```
A: Negative
C: Positive
```

We denote the labels as L_0 and L_1 , so that L_0 is A in the first context and B in the second context. We denote the option texts as O_0 and O_1 .

We perform an experiment where we intervene by copying over a suffix of every line from the source context into the target context, and plot the accuracy based on whether the intervention successfully changes the belief (Fig. 8). The right most point of the plot is the control condition where no interventions are made. The accuracy is near zero because the model currently believes in the original context. At the left most point, we intervene on the entire statement, which is a substitution of the entire Z_{context} . Thus, we observe a near perfect accuracy.

Interestingly, copying over the activations for the tokens corresponding to “active” and the whitespace following it suffices for almost completely changing the belief, despite having a surface token form that is identical at those two tokens (“active <WS>” for both source and target contexts). This suggests that those activations captures the binding information that contains both the label and the option text. This leads to the conclusion that binding information is bound directly at those activations, instead of indirectly via binding IDs.

In contrast, binding ID would have predicted that substituting these two tokens would not have made a difference, because the option activations Z_O should contain only information about the option text and the binding ID, which is identical for our choice of source and target contexts.

F GENERALITY DETAILS

Suppose π is a cyclic shift, say $\pi(0) = 1, \pi(1) = 2, \pi(2) = 0$. Then, we can perform mean interventions based on the cyclic shift on entities as follows:

$$Z_{E_k} \rightarrow Z_{E_k} + b_E(\pi(k)) - b_E(k) = Z_{E_k} + \Delta_E(\pi(k)) - \Delta_E(k).$$

We then expect the belief to follow the same shift, so that the LM believes $E_k \leftrightarrow A_{\pi(k)}$.

Similarly, we can perform mean interventions on attributes as follows:

$$Z_{A_k} \rightarrow Z_{A_k} + b_A(\pi(k)) - b_A(k) = Z_{A_k} + \Delta_A(\pi(k)) - \Delta_A(k).$$

However, this time we expect the belief to follow the inverse shift, i.e. $E_k \leftrightarrow A_{\pi^{-1}(k)}$, which is the same as $E_{\pi(k)} \leftrightarrow A_k$.

As usual, we sample Δ using 500 samples. We perform the intervention using both cyclic shifts over 3 elements, (i.e. π and π^{-1}), and report the mean results over these two shifts.

G GEOMETRY DETAILS

An experimental challenge we face is that we do not have access to the binding ID vectors b_A, b_E themselves, only differences between them, Δ_A, Δ_E . For clarity of exposition we first describe the procedure we would perform if we had access to the binding ID vectors, before describing the actual experiment.

In the ideal case, we would obtain two pairs of binding ID vectors, $[b_E(0), b_A(0)], [b_E(1), b_A(1)]$. Then, we can construct two linear combinations of these two binding ID vectors as candidate binding IDs, $[v_{E_0}, v_{A_0}]$ and $[v_{E_1}, v_{A_1}]$. Now, we can take an $n = 2$ context \mathbf{c} and intervene on each of $Z_{E_0}, Z_{A_0}, Z_{E_1}, Z_{A_1}$ to change their binding IDs to our candidate binding IDs. If the model retains its beliefs, then we infer that the binding IDs are valid.

There two main problems with this procedure. The first is that we only have access to Δ_A and Δ_E and not b_E, b_A . Instead of choosing $[b_E(0), b_A(0)], [b_E(1), b_A(1)]$ as our basis vectors, we can use contexts with $n = 3$ to obtain $[\Delta_E(1), \Delta_A(1)], [\Delta_E(2), \Delta_A(2)]$. These new basis vectors are still linear combinations of binding IDs, and if binding ID vectors do form a subspace, these would be part of the subspace too.

The second problem is that we cannot arbitrarily set the binding ID vector of an activation to another binding ID vector. Instead, we can only add vectors to activations. We thus perform two sets of interventions. We first perform the mean interventions on the second binding ID pair to turn $[b_E(1), b_A(1)]$ into $[b_E(0), b_A(0)]$. At this point, the LM sees two entities with the same binding ID and two attributes with the same binding ID, and is confused. Then, we can add candidate binding vector ID *offsets* to these activations.

More precisely, let η, ν be coefficients for the linear combinations of the basis vectors. Define now $h_A(\eta, \nu) = \eta\Delta_A(1) + \nu\Delta_A(2)$ and $h_E(\eta, \nu) = \eta\Delta_E(1) + \nu\Delta_E(2)$ as the candidate binding vector ID offsets. Then, we add $[h_E(\eta_0, \nu_0), h_A(\eta_0, \nu_0)]$ and $[h_E(\eta_1, \nu_1), h_A(\eta_1, \nu_1)]$ to the respective two pairs of binding IDs, and evaluate if the model has regained its beliefs.

Concretely, the intervention we apply is parameterized by $(\eta_0, \nu_0, \eta_1, \nu_1)$ and are as follows:

$$\begin{aligned} Z_{A_0} &\rightarrow Z_{A_0} - \Delta_A(0) + h_A(\eta_0, \nu_0), & Z_{E_0} &\rightarrow Z_{E_0} - \Delta_E(0) + h_E(\eta_0, \nu_0), \\ Z_{A_1} &\rightarrow Z_{A_1} - \Delta_A(1) + h_A(\eta_1, \nu_1), & Z_{E_1} &\rightarrow Z_{E_1} - \Delta_E(1) + h_E(\eta_1, \nu_1). \end{aligned}$$

We are now interested in the question: if we have coefficients (η_0, ν_0) and (η_1, ν_1) , are the binding vectors constructed from those coefficients valid binding IDs?

In our experiments (Fig. 5), we fix the value of η_0 and ν_0 at varying positions (green circles), and vary η_1 and ν_1 . We plot the mean median-calibrated accuracy. We find that near the green circle, the model is completely confused, responding with near-chance accuracy. This verifies that the erasure step works as intended. In addition, we find that there appears to be a binding metric subspace in that as long as candidate binding IDs are sufficiently far apart, the LM recovers its ability to distinguish between the two, even when candidate binding IDs are outside of the convex hull between the three binding IDs used to generate the basis vectors.